Chemical Engineering Journal 156 (2010) 532–539

Contents lists available at ScienceDirect

Chemical Engineering Journal

journal homepage: www.elsevier.com/locate/cej

Direct synthesis of hydrogen peroxide from H_2/O_2 and oxidation of thiophene over supported gold catalysts

Shuqi Ma[a,b], Gang Li[a,*], Xiangsheng Wang[a]

[a] Department of Catalytical Chemistry and Engineering, State Key Laboratory of Fine Chemicals, Dalian University of Technology, 158-39, Zhongshan Road, Dalian 116012, PR China
[b] School of Physics and Chemistry, Henan Polytechnic University, Jiaozuo 454000, PR China

ARTICLE INFO

Article history:
Received 24 October 2008
Received in revised form 2 April 2009
Accepted 3 April 2009

Keywords:
Hydrogen peroxide
Direct synthesis
Gold catalyst
TS-1
Active species

ABSTRACT

Direct synthesis of hydrogen peroxide from H_2 and O_2 was performed over supported gold catalysts. The catalysts were characterized by means of UV–vis, H_2-TPR, TEM and XPS. Based on the results we conclude that metallic Au is the active species in the direct synthesis of hydrogen peroxide from H_2 and O_2. During preparation process of catalyst by deposition–precipitation with urea, the pH value increased and the gold particle size decreased with increasing the urea concentration. The catalyst prepared with higher urea concentration showed a higher activity and its stability also was efficiently improved. Gold nanoparticles, supported on TiO_2 or Ti contained supports, gave a higher catalytic activity. Thiophene can be efficiently oxidized by hydrogen peroxide synthesized in situ from H_2 and O_2 over Au/TS-1.

1. Introduction

Hydrogen peroxide (H_2O_2), as an environmental friendly oxidant, has been widely used in many industrial areas. Currently, it is mainly consumed for pulp and textile bleaching, chemical synthesis, and wastewater treatment. Recently, growing interest for the application of H_2O_2 in the chemical industry is related to the discovery of titanium silicalite molecular sieve TS-1 and its application in selective oxidation processes such as the epoxidation of propene, the ammoxidation of cyclohexanone and the hydroxylation of phenol.

Current processes for the production of H_2O_2 are mainly based on a sequential process of hydrogenation and oxidation of an alkylanthraquinone. However, the anthraquinone process has several obvious drawbacks, including complex operation steps, organic waste and safety issues in transportation and storage, and therefore it is not economical in the fine chemical industry, which requires relatively small amounts of hydrogen peroxide at one time. Consequently, alternative routes for H_2O_2 synthesis are highly desirable.

Direct synthesis of H_2O_2 from H_2 and O_2 is a more economic, simple and environmental friendly process. This direct route was first discovered by Henkel and Weber [1] in 1914, and in recent years has received large attention due to the increasing demands for H_2O_2. Extensive studies based on supported palladium (Pd) catalysts have been performed in the past decades [2]. Recently, supported gold nanoparticles are proved to be potential catalysts for the direct formation of H_2O_2 from H_2 and O_2. Landon et al. [3–6] reported that gold catalysts supported on metal oxides, such as ZnO, CeO_2, Al_2O_3, TiO_2, and Fe_2O_3, were efficient for the direct formation of H_2O_2 from H_2 and O_2 in a mixture of methanol and water as reaction medium. Okumura et al. [7] investigated the direct synthesis of H_2O_2 and found a higher rate of H_2O_2 production obtained over SiO_2, MCM-41 and active carbon-supported gold catalysts prepared by gas-phase grafting. Zeolite HZSM-5 and Y-supported Au catalysts were used by Li et al. [8] to directly synthesize hydrogen peroxide, and similar rates were obtained as over alumina and silica-supported Au catalysts. Ishihara et al. [9] studied the direct synthesis of H_2O_2 from H_2 and O_2 over Au/SiO_2 in detail.

Over supported Pd catalysts, the effect of the Pd oxidation state on the direct synthesis of H_2O_2 has been investigated by many groups. Based on the productivity and selectivity of H_2O_2, Choudhary et al. [10,11] have claimed that a PdO catalyst is more suitable than a Pd^0 catalyst. On the contrary, some scientists, including Thompson and co-workers [12], Chinta and Lunsford [13], and Burch and Ellis [14], have claimed that Pd^0 catalysts have a higher H_2O_2 productivity and selectivity. Dissanayake and Lunsford [15] have demonstrated that colloidal palladium is an active phase for the formation of H_2O_2 from H_2 and O_2 in an HCl-acidified-aqueous medium. However, over supported gold catalysts, the Au active phase in the direct synthesis of H_2O_2 is still not clear.

Based on the unique catalytic activity of TS-1 molecular sieve in many selective oxidation processes, integrating the direct synthesis of H_2O_2 from H_2/O_2 with the oxidative reactions catalyzed by TS-1 will be a very interesting strategy. In these processes, the

---

* Corresponding author. Tel.: +86 411 83689065; fax: +86 411 83689065.
E-mail address: liganghg@dlut.edu.cn (G. Li).

1385-8947/$ – see front matter © 2009 Elsevier B.V. All rights reserved.
doi:10.1016/j.cej.2009.04.004

in situ generated H_2O_2 will be selectively transferred to the substrate, and therefore the utilization will be more efficient compared with the commercial H_2O_2. TS-1 supported Au catalysts have been used in gas phase epoxidation of propylene in the presence of H_2 and O_2, and H_2O_2 or surface hydroperoxy species formed over the supported Au surface were proposed as the oxidative intermediate [16].

Some studies have reported [17–19] that sulfides, such as thioether, thiophene and methyl-thiophene, can also be efficiently oxidized over TS-1, using hydrogen peroxide as oxidant. As the primary organic sulfur of the commercial gasoline, the oxidative removal of thiophene over TS-1 is a very promising step to obtain ultra-low sulfur gasoline. In this paper, we present a detailed investigation of the direct synthesis of H_2O_2 over supported gold catalysts, and the gold active phase is discussed. Using TS-1 supported gold catalysts, the oxidation of thiophene by H_2O_2 generated in situ is also studied.

2. Experimental

2.1. Catalyst preparation

The titanium silicalite TS-1 support was prepared according to a reported procedure [20]. Colloidal silica (30%) and tetra-butyl-orthotitanate (TBOT) were used as silicon and titanium source, respectively. Tetrapropylammonium bromide (TPABr) and n-butylamine were used as the template and the base. TS-1 samples crystallized from gels with the following molar composition: $SiO_2 - a \times TiO_2 - b \times$ n-butylamine $- c \times$ TPABr $- d \times H_2O$, where $0 < a < 0.03$, $0 < b < 1.0$, $0 < c < 0.1$ and $20 < d < 100$. The gel was transferred into an auto-clave and heated at 150–190 °C for 2–10 days. The slurry was filtered, washed with distilled water and dried at 100 °C in static air, and finally calcined at 540 °C for 6 h. Other supports, TiO_2 (Deggusa P25), Al_2O_3 (SB powder) and SiO_2 (silica fume), were also used.

Gold was deposited on the support by a homogenous deposition precipitation (HDP) method using urea as precipitator. In a typical catalyst preparation for 2 wt% Au/TS-1, 1 g TS-1 was suspended in 50 mL aqueous solution of $HAuCl_4$ (2.03×10^{-3} M). Excess urea was added, and the initial pH value was about 2. The temperature of suspension was maintained at 80 °C for 3 h under vigorous stirring and then aged at 30 °C for 3 h. The solid was collected by centrifugation, washed 6–7 times with distilled water in the centrifuge tube with 15 mL capacity, dried in air at ambient temperature. The as-made material was calcined in static air at a heating rate of 2 °C min^{-1} from ambient temperature to 400 °C and maintained at the final temperature for 4 h. Other catalysts, namely Au/TiO_2, Au/Al_2O_3 and Au/SiO_2, were also prepared by the HDP method.

2.2. Catalytic tests

The synthesis of hydrogen peroxide was performed in a jacketed stainless autoclave with Teflon liner and a nominal volume of 100 mL. The autoclave was equipped with a magnetic stirrer, a water bath jacket, and provisions for measuring the pressure of the charging gases. The reaction temperature was controlled by a water bath. Typically, catalysts and reaction medium were fed into the reactor, purged three times with inert N_2 (0.2 MPa), and then charged with H_2/N_2 and O_2/N_2 mixed gas mixtures to give a H_2 partial pressure of 0.3 MPa and an oxygen-to-hydrogen ratio of 3:1 at a total pressure of 1.5 MPa. The reaction was run with magnetic stirring at ambient temperature (25 °C unless otherwise stated). The reaction was run for 2 h and the H_2O_2 concentration was determined by iodometric titration.

For oxidative desulfurization reaction, thiophene was dissolved in n-octane as model gasoline. The content of thiophene was about 268 ppm (100 μg/g S) and de-ionized water was used as solvent. The oxidation of thiophene was performed under similar conditions as the synthesis of hydrogen peroxide. For addition, 10 mL model gasoline (thiophene in n-octane) was added. The contents of thiophene before and after reaction were analyzed by means of an Agilent-6890 gas chromatograph equipped with a flame photometric detector (FPD) and HP-5 capillary column.

2.3. Catalyst characterization

Diffuse reflectance UV–vis spectroscopy (DR/UV–vis) experiments have been performed using a Jasco V-550 spectrophotometer. The measurements were performed using air-exposed samples between 190 and 850 nm. The actual loading of gold on TS-1 was determined by means of inductively coupled plasma atom emission spectroscopy (ICP-AES) on a Plasam-Spec-I (Leem Labs, USA). TEM measurements were performed using a Phillips Tecnai G2 20 microscope with a CCD camera operated at 180 kV.

TPR was performed using a lab-scale setup specially designed for this purpose, with a thermal conductivity detector (TCD) for gas analysis. Prior to each experiment, 0.1 g of the sample was pretreated at 100 °C in an N_2 flow for 1 h in order to remove the surface contaminants and physically absorbed water. After cooling to room temperature under N_2, the gas flow was switched to 7.85 vol% H_2/N_2 at a total flow rate of 40 mL/min, and heated at a raise rate of 10 °C min^{-1} to a final temperature of 800 °C.

X-ray photoelectron spectra (XPS) were recorded at room temperature on a KRATOS AMICAS spectrometer (Shimadzu, Japan) using a Mg Kα ($h\nu = 1253.6$ eV) X-ray source. Samples were pressed into pellets and mounted using double-sided adhesive tape, and all binding energies were calibrated using contaminant carbon ($C_{1s} = 284.6$ eV) as the reference. The background pressure during data acquisition was kept below 1.5×10^{-6} Pa. Background subtraction and peak fitting were performed using the XPSPEAK 4.0 peak fitting program. The peak area of full width at half-maximum (FWHM) and the position of Au 4f component were unconstrained in all fits. The separation between the spin–orbit coupled peaks Au $4f_{7/2}$ and Au $4f_{5/2}$ was set to 3.7 eV. The relative areas of the Au $4f_{7/2}$ and Au 4f $_{5/2}$ peaks were fixed at a ratio of 4:3, while their FWHM were fixed at a ratio of 1:1.

3. Results and discussion

3.1. Direct synthesis of H_2O_2

3.1.1. Influence of calcination temperature of Au/TS-1

It is generally known that, over supported gold catalysts, the gold oxidation state and the gold particle size are influenced by the calcination temperature. Here, we investigated the influence of the calcination temperature on the catalytic activity of the Au/TS-1 catalysts in the direct synthesis of H_2O_2. These as-made Au/TS-1 samples, which had been dried at ambient temperature, were treated at different temperatures, namely 100, 200, 300, 400, 500 or 600 °C. No hydrogen peroxide can be formed over the two samples dried at ambient and 100 °C. With increasing temperature of calcinations from 200 to 600 °C, an increase in the catalytic activity could be first observed, and when the calcination temperature was above 400 °C, the catalytic activity began to decrease (Fig. 1).

Fig. 2 shows the TEM images of 2 wt% Au/TS-1 catalysts calcined at 200, 400, 600 °C. The spherical gold particles (black dots in Fig. 2) are fairly distributed on the support surface. Based on more than 500 particles in these TEM images, the average gold particle sizes were calculated to be 7.1, 12.3 and 26.7 nm for these samples

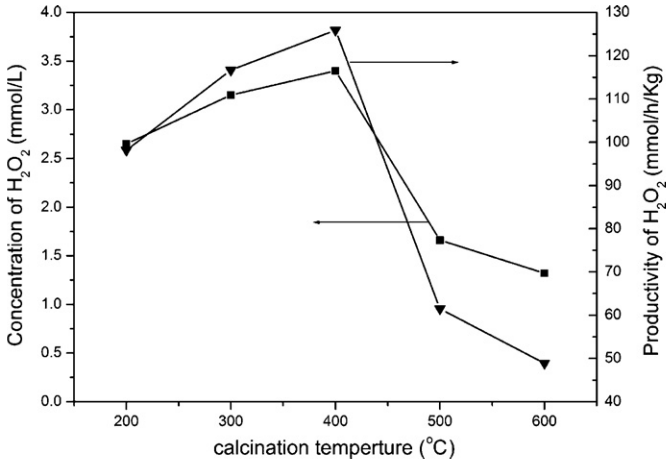

Fig. 1. Direct synthesis of H_2O_2 over Au/TS-1 catalysts calcined at different temperatures. Reaction conditions: 0.135 g catalyst, 10 mL de-ionized water, $H_2/N_2/O_2$ = 1:1:3, total pressure 1.5 MPa, 25 °C, 2 h.

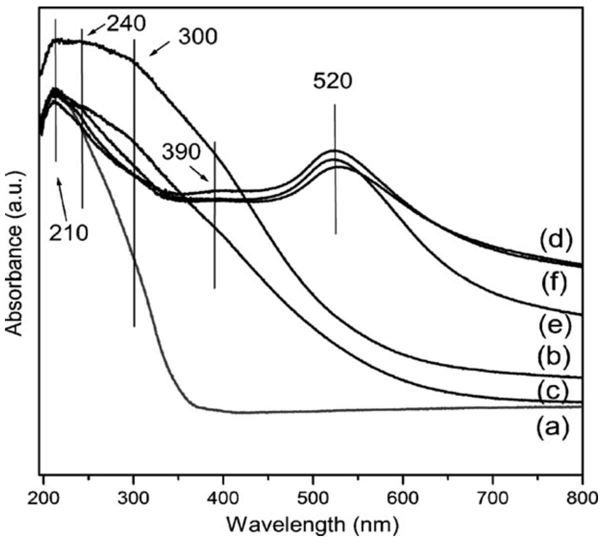

Fig. 3. UV–vis spectra of Au/TS-1 catalysts treated at different temperatures: (a) TS-1, (b) ambient temperature, (c) 100 °C, (d) 200 °C, (e) 400 °C, (f) 500 °C.

calcined at 200, 400 and 600 °C, respectively. Furthermore, the gold particles have a much broader size distribution with increasing calcination temperature. These results indicate that agglomeration of gold particles has taken place with increasing calcination temperature.

In Fig. 3, the UV–vis spectra of the TS-1 support and the 2 wt% Au/TS-1 catalysts treated at different temperatures are illustrated. For the TS-1 molecular sieve, only an absorption peak around 210 nm, which is attributed to the tetrahedrally coordinated framework Ti species, can be observed, and no absorption peaks of octahedral Ti species and anatase could be detected around 240 and 330 nm, respectively [21]. All these Au/TS-1 catalysts also exhibit the absorption peak of framework Ti around 210 nm. The Au/TS-1 catalysts dried at 40 and 100 °C show another two peaks around

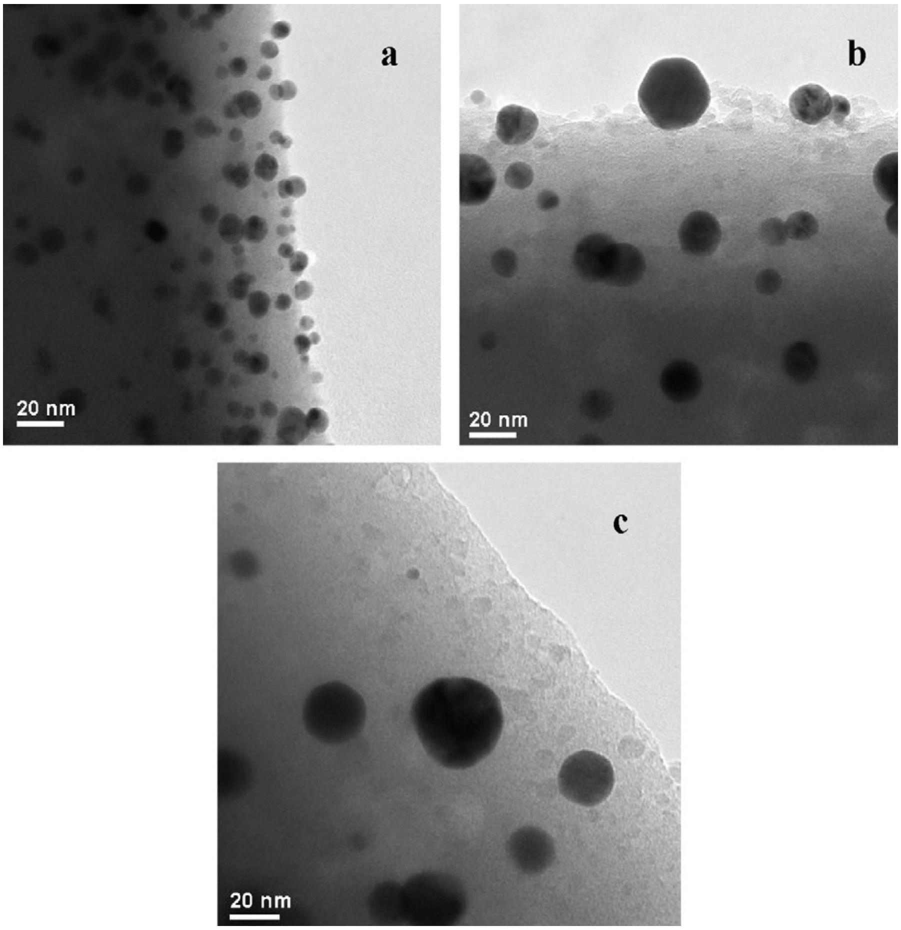

Fig. 2. TEM images of Au/TS-1 calcined at different temperatures: (a) 200 °C, (b) 400 °C, (c) 600 °C.

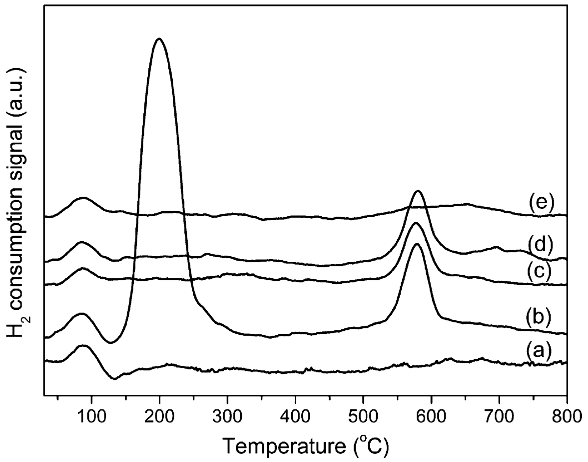

Fig. 4. TPR profiles of Au/TS-1 treated at different temperatures: (a) TS-1 support, (b) dried at 100 °C, and calcined at (c) 200 °C, (d) 400 °C, (e) 600 °C.

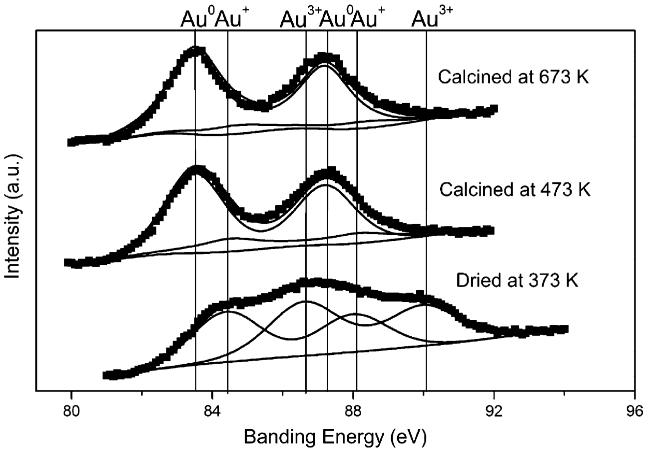

Fig. 5. XPS spectra of Au/TS-1 treated at different temperatures.

240 and 300 nm. Several reported literature [22,23] have attributed these two peaks to the absorption peaks of Au^+ and Au^{3+}, respectively. After calcined at 200 °C, the typical plasmon peak of metallic gold around 520 nm appears, and the peak around 300 nm disappears. With increasing temperature of calcination, the intensity of the peak around 520 nm increases, and the peak around 240 nm becomes much weaker, and disappears after the catalyst calcined at 500 °C. A absorption peak at 390 nm, corresponding to the plasmon resonance of $(Au)_n{}^{\delta+}$ [24], also appears for the samples calcined at 200–500 °C. This slightly oxidized species may be formed from the interaction between metallic gold and lattice oxygen. These results reveal that the gold species are auto-reduced to metallic state by increasing the calcination temperature.

For these samples calcined at 200, 400, 500 °C, the peak around 520 nm shows different shape, defined here as the FWHM of the peak, and has a shift to lower wavelength with increasing calcination temperature. The variation of FWHM and the blue shift have been explained in terms of the difference in the size of the gold particles by some scientists [23]. They have proved that, when the mean diameter of the gold particles is smaller than 25 nm, the absorption peak position shifts to the lower wavelength and the FWHM decreases with increasing the size of the Au nanoparticles. Therefore, with increasing temperature of calcination, the Au/TS-1 catalysts have a higher gold particle size. This observation has been confirmed by the TEM characterization.

Fig. 4 shows the H_2-TPR profiles of unsupported TS-1 and Au/TS-1 catalysts calcined at increasing temperatures. TS-1 and all Au/TS-1 samples exhibit a low temperature reduction peak around 85 °C. According to the literature [25,26], we assign this peak to the reduction of oxygen species on the surface of Ti^{4+}. In the profile of the Au/TS-1 sample dried at 100 °C (Fig. 4(b)), an intense reduction peak is detected around 190 °C, and this peak disappears for the catalysts calcined at a temperature above 200 °C. This peak should be assigned to the reduction of oxidic gold species. For the samples calcined at 100, 200, and 400 °C, another reduction peak is presented around 565 °C. We attribute this peak to the reduction of $Au^{\delta+}$ in the internal structure of TS-1. This gold species is incorporated in the subsurface of TS-1 and therefore it still cannot be completely reduced by calcined at 400 °C. This peak disappears when the catalyst is calcined at 600 °C, showing that all gold species were auto-reduced to metallic Au^0, when the sample was calcined at 600 °C.

XPS spectra of Au 4f for those catalysts calcined at increasing temperatures are shown in Fig. 5. Each gold species shows two peaks, due to the Au $4f_{7/2}$ and Au $4f_{5/2}$ transitions. The XPS spectroscopy of Au/TS-1 dried at 100 °C shows two Au 4f binding energies (BE) peaks at 84.6 and 86.7 eV, attributed to oxidic Au^+ and Au^{3+} gold species [27], respectively. The Au/TS-1 samples calcined at 200 and 400 °C have a dominant Au 4f BE of 83.5 eV, assigned to metallic Au species. This suggests that metallic Au^0 is mainly Au species on these two samples. In Table 1 data obtained by XPS analysis for Au, Ti and Si are summarized. The gold species and relative concentration on the surface of Au/TS-1 calcined at different temperatures are listed. These data confirm that Au^+ and Au^{3+} are main gold species on the sample dired at 100 °C and they are gradually auto-reduced to metallic Au^0 with increasing calcination temperature. The BE of Ti 2p at 459.3 eV is due to tetrahedrally coordinated Ti^{4+} species, and Si 2p shows only one BE at 533.1 eV. The surface atomic ratio of Au/Ti decreases from 2.83 to 0.53 with the calcination temperature increasing from 100 to 400 °C. The atomic ratio of Au/Si also decreases when the calcination temperature increase from 100 to 200 °C, but it is equal for the samples calcined at 200 and 400 °C. With increasing calcination temperature, the TEM characterization has proved that the gold particles agglomerate to have a higher particle size. Therefore, more Ti and Si species expose on the surface of Au/TS-1, and this explains the reason why the surface atomic ratio of Au/Ti and Au/Si decrease. The higher decrease rate for the surface atomic ration of Au/Ti than that of Au/Si and the equal Au/Si ratios for the samples calcined at 200 and 400 °C can be explained by that Au particles prefer to selectively deposit on Ti sites than Si sites. Haruta et al. [28] also have proved this.

According to UV–vis, TPR and XPS, Au^+ and Au^{3+}, which are mainly gold species on the Au/TS-1 catalysts dried at 40 and 100 °C, cannot catalyze H_2/O_2 to form H_2O_2. The increasing catalytic activity at higher calcination temperature from 200 to 400 °C can be explained by the gradual reduction of gold species to metallic Au^0. When the calcination temperature exceeding 400 °C, the further increase of the Au particle size results into the rapidly decrease of the catalytic activity.

3.1.2. pH value during precipitation

Using urea as the precipitator, Zanella et al. [29] found that, with increasing the DP time, the increase of pH value of the solution could result in changes in the surface charge density of the gold precipitate particles, and lead to a fragmentation of the particles, and therefore the gold particle size decreased. Here, we investigated the effect of the urea concentration on the pH value of the solution, the gold particle size, and finally on the catalytic activity of Au/TS-1.

Table 2 shows the catalytic activity of Au/TS-1 catalysts which had been precipitated with different urea concentrations. The catalyst which was precipitated with 0.27 mol/L urea gives the lowest

Table 1
XPS analysis of Au/TS-1 pretreated at different temperatures.

Calcination temperature (°C)	BE Au $4f_{7/2}$ (eV)		BE Ti 2p (eV)	BE Si 2p (eV)	Au/Ti	Au/Si
100	84.6 Au^+ 86.7 Au^{3+}	[46.8][a] [53.2]	459.3	533.1	2.83	0.12
200	83.5 Au^0 84.7 Au^+	[81.1] [18.9]	459.2	533.0	0.78	0.061
400	83.5 Au^0 84.7 Au^+	[88.6] [11.4]	459.1	532.9	0.53	0.058

[a] The relative concentration of two Au species in square brackets.

Table 2
Direct synthesis of H_2O_2 over 2 wt% Au/TS-1 prepared with different concentration of urea.

Content of urea (mol/L)	Productivity (mol H_2O_2/(kg$_{cat}$ h))	Concentration of H_2O_2 (mmol/L)
0.27	0.64	1.60
0.33	1.14	2.85
0.4	1.65	4.12
0.5	1.96	4.90

Reaction conditions: 50 mg catalyst, 10 mL de-ionized water, $H_2/N_2/O_2$ = 1:1:3, total pressure 1.5 MPa, 25 °C, 30 min.

activity in the direct synthesis of H_2O_2 from H_2 and O_2. The productivity and the concentration for H_2O_2 are 0.64 mol/(kg$_{cat}$ h) and 1.60 mmol/L, respectively. The catalytic activity increases with increasing the concentration of urea. The concentration of H_2O_2 increases from 1.60 to 4.12 mmol/L when the urea concentration increases from 0.27 to 0.40 mol/L. Further increasing urea concentration, the H_2O_2 concentration only has a slightly increase. In Fig. 6, the TEM images are showed. The catalyst prepared with 0.27 mol/L urea exhibits the highest average particle size of 12.3 nm. With increasing urea concentration, the catalyst shows a more homogenous dispersion of gold particles and a smaller particle size. Fig. 7 shows the effect of the urea concentration on the average particle size and the pH value of solution. With increasing the urea concentration, an increase trend in pH value and a decrease trend in particle size can be distinctly seen and the smaller gold particles are beneficial to synthesize H_2O_2.

The stability of heterogeneous catalyst is a key factor for the multi-phase reaction. The reuse of the catalysts, prepared with 0.33 and 0.40 mol/L urea, was performed (Fig. 8). Before each reuse, the catalyst was washed 3 times with water to eliminate H_2O_2 that was possible adsorbed on the catalysts. ICP-AES analysis was used to detect the change of gold content during reuse. For the catalyst prepared with 0.33 mol/L urea, the gold content had a loss of 50% from 2.2 wt% before initial use to 1.1 wt% after fourth time, and the H_2O_2 productivity also decreased from 1.2 to 1.0 mol/(kg$_{cat}$ h). To prove whether the species leached into the reaction medium

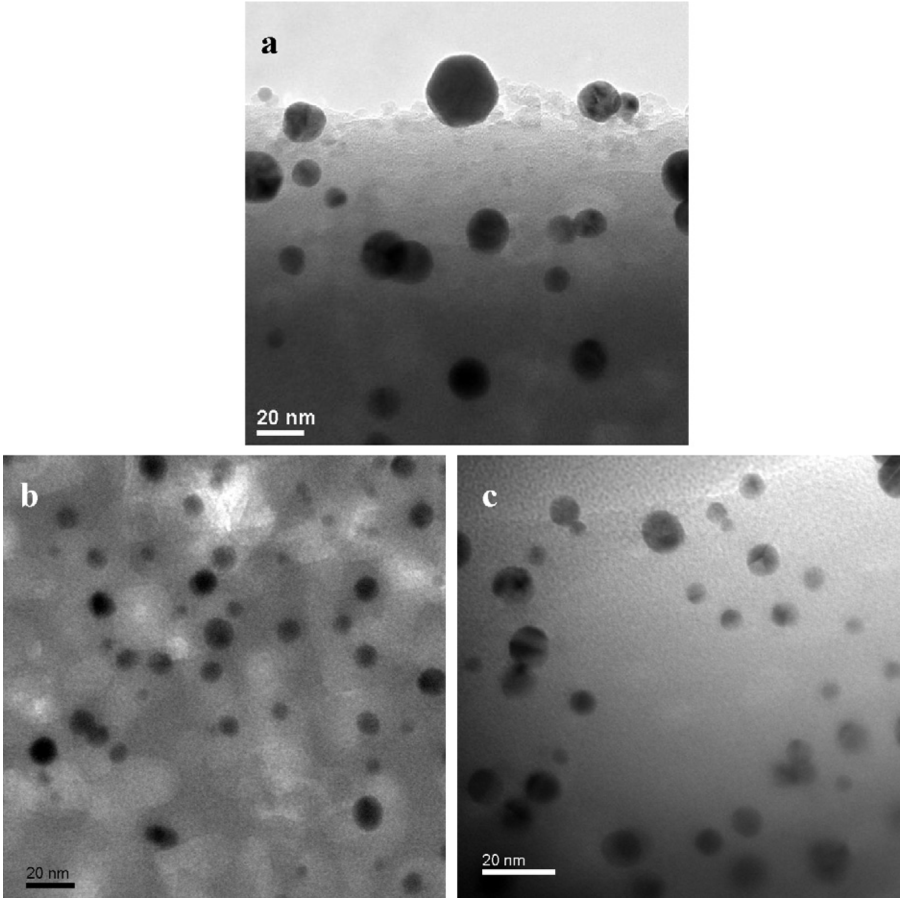

Fig. 6. TEM images of Au/TS-1 prepared under different contents of urea: (a) 0.27 mol/L, (b) 0.4 mol/L, (c) 0.5 mol/L.

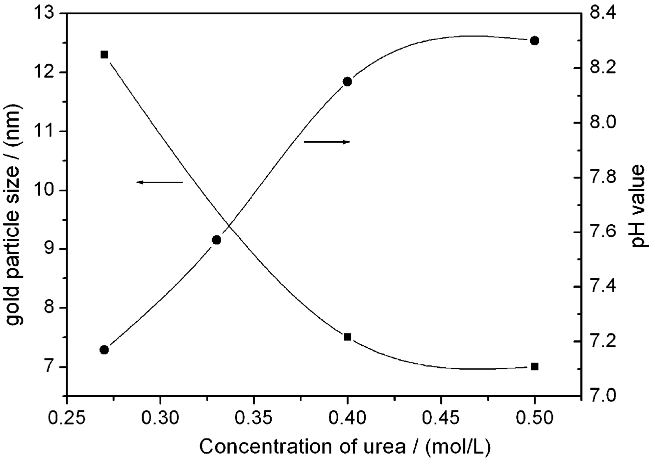

Fig. 7. Effect of the urea concentration on gold particle size and pH value of the solution.

is active for the direct synthesis of hydrogen peroxide, we carried out two experiments. First, following the initial use, the catalyst was removed by centrifugation, and the solution was used again in the presence of H_2 and O_2. No H_2O_2 was further formed. Second, the Au/TS-1 catalyst was washed with water to leach the gold species, and then the solution was used for the synthesis of H_2O_2. No hydrogen peroxide was formed either. These results proved that the gold species leached from the catalyst is not active for the synthesis of hydrogen peroxide. The catalyst is a truly heterogeneous catalyst in the process. But the catalyst prepared with 4.0 mol/L urea only had a slight decrease of gold content from 2.4 to 2.0 wt%, and its activity nearly did not decrease during reuse. So, in the precipitation process of gold particles, adequate amount urea and/or pH value is necessary to obtain catalyst with higher activity and stability.

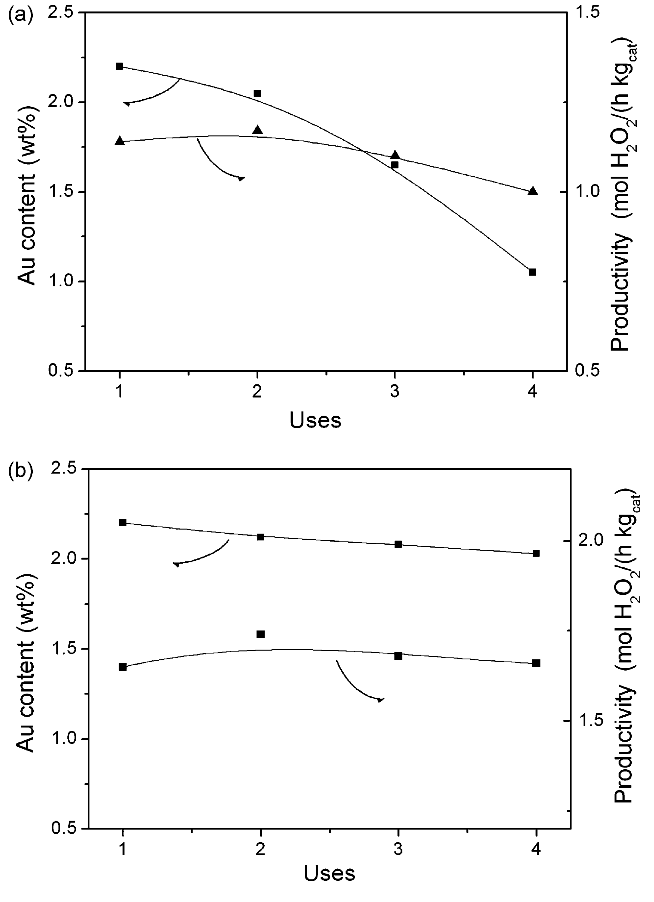

Fig. 8. Reuse of Au/TS-1 in the direct synthesis of H_2O_2 over Au/TS-1 prepared under the content of urea (a) 0.33 mol/L, and (b) 0.4 mol/L. Reaction conditions: 50 mg catalyst, 10 mL de-ionized water, $H_2/N_2/O_2$ = 1:1:3, total pressure 1.5 MPa, 25 °C, 30 min.

3.1.3. *Influence of support*

The nature of the support as well as the physical state can influence the catalytic activity of supported gold catalyst. The catalytic activity of gold supported TiO_2, TS-1, Al_2O_3 and SiO_2 was studied in the direct synthesis H_2O_2 from H_2 and O_2 (Table 3). The samples were prepared by DP urea. Under the same reaction conditions, the gold catalysts supported on the support containing Ti, namely TiO_2 and TS-1, show higher activity than Al_2O_3. Au/SiO_2 catalyst, prepared by DP urea, could not catalyze H_2 and O_2 to form H_2O_2. Nevertheless, Okumura et al. [7] prepared highly dispersed small gold particles on SiO_2 by gas-phase gifting, which showed a high catalytic activity in the direct synthesis of H_2O_2. Two another groups [5,9] also showed that the Au/SiO_2 catalyst prepared by incipient wetness had a considerable catalytic activity in this reaction. These indicate that the reason for the low catalytic activity of the Au/SiO_2 cannot be simply attribute to the nature of the support, but that the preparation method is crucial. Compared the iso-electric point (IEP) of the supports, the supports of active gold catalysts have an IEP between 6 and 9, and the IEP of SiO_2 is 2. The DP method is not applicable to metal oxides, the IEPs of which are below 5. In the pH range needed to precipitate $Au(OH)_3$ the highly negatively charged surface of SiO_2 does not allow the adsorption of $[Au(OH)_nCl_{4-n}]^-$ species onto the support surface, which is necessary for the formation and stabilization of small gold particles [30].

Fig. 9 shows the TEM images of Au/TiO_2, Au/TS-1, Au/Al_2O_3 and Au/SiO_2. Au/TiO_2 and Au/Al_2O_3 have similar gold particle sizes and average gold particle size is about 3–4 nm. The gold particles have an average size of 7.5 nm with size distribution from 3–15 nm on TS-1, and the size of all gold particles is above 25 nm on SiO_2. Comparing the similar gold particle sizes, the activity of Au/TiO_2 is higher than that of Au/Al_2O_3. This indicates that the catalytic activity is influenced by not only the gold particle size but also the nature of the support.

Table 3 also shows the effect of the catalyst weight and the reaction medium on the direct synthesis of H_2O_2. With increasing catalyst weight, the concentration of H_2O_2 synthesis increased. When the 50 mg Au/TS-1 was used, the concentration of H_2O_2 synthesized from H_2/O_2 in 30 min was 4.12 mmol/L, while it was 2.45 mmol/L when 10 mg catalyst was used. However, the productivity of H_2O_2 was higher at lower catalyst weight. This can be explained by the primary reactions happening in the direct synthesis of H_2O_2. Besides the ability to catalyze the synthesis of H_2O_2 from H_2 and O_2, the catalysts can also catalyze the decomposition and hydrogenation of H_2O_2. Fig. 10 shows that about 59.4% H_2O_2 was decomposed in the presence of Au/TS-1 catalyst, twice times higher than that in the presence of unsupported TS-1 molecular sieve. Besides the decomposition of H_2O_2, the Au/TS-1 catalyst can also catalyze the hydrogenation of H_2O_2. When H_2 was charged, the decomposition of H_2O_2 was about 83.9%. With increasing catalyst weight, the rate of H_2O_2 decomposition also increased, and therefore, the productivity of H_2O_2 decreased. Because the solubility of H_2 and O_2 is higher in methanol than in water, the disadvantageous influence of mass transfer is depressed. Therefore, higher H_2O_2 productivity was obtained in the methanol medium. It is 5.96 mmol/(kg_{cat} h) in methanol for the Au/TiO_2 catalyst, almost three times higher than that in water.

Table 3
Direct synthesis of hydrogen peroxide over different gold catalysts.

Catalyst	Catalyst weight (mg)	Solvent	Productivity (mol H_2O_2/(kg_{cat} h))	Concentration (mmol/L)
Au/TiO_2	50	Water	2.04	5.10
Au/TiO_2	50	Methanol	5.96	14.90
Au/TS-1	50	Water	1.65	4.12
Au/TS-1	10	Water	4.90	2.45
Au/SiO_2	50	Water	0	0
Au/Al_2O_3	50	Water	0.63	1.57

Reaction conditions: 2 wt% Au/support, 50 mg catalysts, 10 mL de-ionized water, $H_2/N_2/O_2$ = 1:1:3, total pressure 1.5 MPa, 25 °C, 30 min.

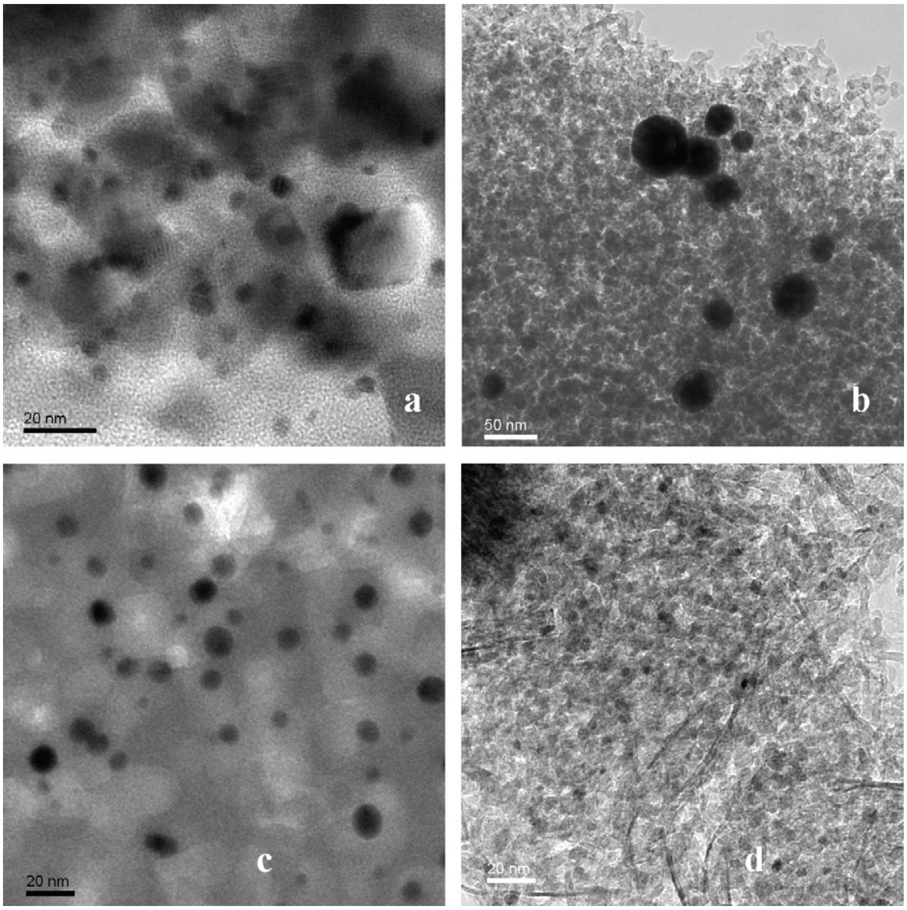

Fig. 9. TEM images of gold catalysts supported by different supports: (a) Au/TiO_2, (b) Au/SiO_2, (c) Au/TS-1, (d) Au/Al_2O_3.

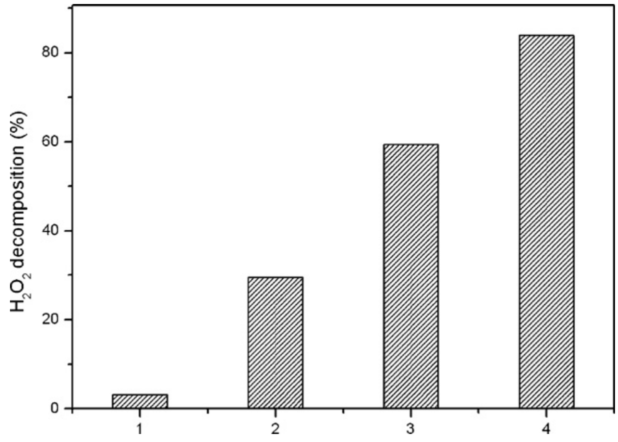

Fig. 10. Decomposition of hydrogen peroxide over Au/TS-1: (1) no catalyst, (2) TS-1, (3) Au/TS-1, (4) Au/TS-1 and 0.3 MPa H_2 charged. Reaction conditions: 0.135 g Au/TS-1, 10 mL H_2O_2 solution with a concentration of 9.3 mmol/L, 25 °C, 1 h.

3.2. *Oxidation of thiophene*

Using hydrogen peroxide as oxidant, thiophenic sulfides can be efficiently oxidized over titanium silicalite TS-1. We investigated the catalytic activity of Au/TS-1 in the oxidation of thiophene in the presence of H_2 and O_2.

Table 4 shows the effect of reaction time and reaction temperature. The removal of thiophene increases with increasing reaction time. After 6 h, about 100% removal of thiophene could be achieved. In our earlier report [31], we proved that thiophene can neither be oxidized over TS-1 in the presence of H_2 and O_2, nor over Au/TS-1 in the presence of only O_2. These results reveal that thiophene can be efficiently removed by hydrogen peroxide continually synthesized in situ from H_2 and O_2 over Au/TS-1.

Low temperature is beneficial for the formation of hydrogen peroxide [31]. However, thiophene is more easily oxidized at higher temperature [18]. The effect of reaction temperature is shown in Table 4. The removal of thiophene is higher when reaction temperature is above ambient, and the highest removal is 88% at 40 °C.

Table 4
Oxidation of thiophene over Au/TS-1 in the presence of H_2 and O_2.

Reaction time (h)	Reaction temperature (°C)	Removal (%)
2	25	73.0
4	25	89.0
6	25	100
2	40	88.3
2	60	79.8
2	80	81.2

Reaction conditions: 0.135 g 2 wt% Au/TS-1 (calcined at 400 °C), 10 mL de-ionized water, 10 mL model gasoline, $H_2/N_2/O_2$ = 1:1:3, total pressure 1.5 MPa.

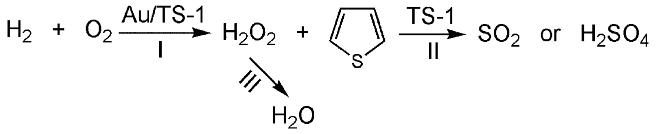

Scheme 1. Oxidation of thiophene over Au/TS-1 in the presence of H_2 and O_2.

Main reactions included in this system are shown in Scheme 1. Increasing reaction temperature favors not only the oxidation of thiophene (reaction II), but also the decomposition of hydrogen peroxide (reaction III). There is a competition between reaction II and III.

After reaction, the water phase is slightly acidic, and a white suspended floc of $BaSO_4$ can be obtained by adding $Ba(NO_3)_2$ solution to the water phase. The results are in accordance with our earlier research on thiophene oxidation over TS-1/H_2O_2 [18]. In that report, we proved that thiophene can be converted into sulfuric acid and/or into sulfur dioxide when insufficient H_2O_2 is provided over TS-1/H_2O_2.

4. Conclusion

Various characterization techniques indicate that the active state of Au is metallic Au^0 in the direct synthesis of hydrogen peroxide from H_2 and O_2 over supported gold catalysts. When the urea concentration increases during the preparation process, the gold particles obtained after calcination exhibit a decreasing size, so catalytic activity and stability of the catalysts can be efficiently promoted. Gold catalysts, supported on TiO_2 or Ti contained support, gave a higher catalytic activity. SiO_2 was not a suitable support to prepare gold catalyst by the method of deposition–precipitation. The Au/SiO_2 catalyst prepared by HDP could not catalyze H_2 and O_2 to form hydrogen peroxide. Comparing two samples with similar gold particle sizes, Au/TiO_2 exhibited a higher activity than Au/Al_2O_3. This indicates not only that the catalytic activity is a particle size effect, but also that the nature of the support should play an important role. Integrating the synthesis of H_2O_2 and oxidation of thiophene over the bifunctional Au/TS-1 catalyst, thiophene can be efficiently oxidative removed in the presence of H_2 and O_2.

Acknowledgements

The financial support of The Foundation for the Author of the National Excellent Doctoral Dissertation of PR China (No. 200346), the Program for New Century Excellent Talents in University (NCET-04-0270), National Natural Science Foundation of China (No. 20406005) and the Scientific Research Foundation for Returned Overseas Chinese Scholars of the State Education Ministry is gratefully acknowledged.

References

[1] H. Henkel, W. Weber, US Patent No. 1,108,752 (1914).
[2] J.M. Campos-Martin, G. Blanco-Brieva, J.L.G. Fierro, Angew. Chem., Int. Ed. 45 (2006) 6962–6984.
[3] P. Landon, P.J. Collier, A.J. Papworth, C.J. Kiely, G.J. Hutchings, Chem. Commun. (2002) 2058–2059.
[4] P. Landon, P.J. Collier, A.F. Carley, D. Chadwick, A.J. Papworth, A. Burrow, C.J. Kiely, G.J. Hutchings, Phys. Chem. Chem. Phys. 5 (2003) 1917–1923.
[5] J.K. Edwards, B.E. Solsona, P. Landon, A.F. Carley, A. Herzing, C.J. Kiely, G.J. Hutchings, J. Catal. 236 (2005) 69–79.
[6] B.E. Solsona, J.K. Edwards, P. Landon, A.F. Carley, A. Herzing, C.J. Kiely, G.J. Hutchings, Chem. Mater. 18 (2006) 2689–2695.
[7] M. Okumura, Y. Kitagawa, K. Yamagcuhi, T. Akita, S. Tsubota, M. Haruta, Chem. Lett. 32 (2003) 822–823.
[8] G. Li, J. Edwards, A.F. Carley, G.J. Hutchings, Catal. Today 114 (2006) 369–371.
[9] T. Ishihara, Y. Ohura, S. Yoshida, Y. Hata, H. Nishiguchi, Y. Takita, Appl. Catal. A 291 (2005) 215–221.
[10] A.G. Gaikwad, S.D. Sansare, V.R. Choudhary, J. Mol. Catal. A: Chem. 181 (2002) 143–149.
[11] V.R. Choudhary, A.G. Gaikwad, S.D. Sansare, Catal. Lett. 83 (2002) 235–239.
[12] V.V. Krishnan, A.G. Dokoutchaev, M.E. Thompson, J. Catal. 196 (2000) 366–374.
[13] S. Chinta, J.H. Lunsford, J. Catal. 225 (2004) 249–255.
[14] R. Burch, P.R. Ellis, Appl. Catal. B: Environ. 42 (2003) 203–211.
[15] D.P. Dissanayake, J.H. Lunsford, J. Catal. 214 (2003) 113–120.
[16] A.K. Sinha, S. Seelan, S. Tsubota, M. Haruta, Topics Catal. 29 (2004) 95–102.
[17] Y. Shiraishi, T. Hirai, I. Komasawa, J. Chem. Eng. Jpn. 35 (2002) 1305–1311.
[18] L.Y. Kong, G. Li, X.S. Wang, Catal. Lett. 92 (2004) 163–167.
[19] L.Y. Kong, G. Li, X.S. Wang, Catal. Today 93–95 (2004) 341–345.
[20] G. Li, X.W. Guo, X.S. Wang, Q. Zhao, X.H. Bao, X.W. Han, L.W. Lin, Appl. Catal. A 185 (1999) 11–18.
[21] G.N. Vayssilov, Catal. Rev. Sci. Eng. 39 (1997) 209–251.
[22] J.L. Margitfalvi, A. Fási, M. Hegedűs, F. Lónyi, S. Gőbölös, N. Bogdanchikova, Catal. Today 72 (2002) 157–169.
[23] S. Link, M.A. El-Sayed, J. Phys. Chem. B 103 (1999) 4212–4217.
[24] A.C. Gluhoi, X. Tang, P. Marginean, B.E. Nieuwenhuys, Topics Catal. 39 (2006) 101–110.
[25] V. Idakiev, L. Ilieva, D. Andreeva, J.L. Blin, L. Gigot, B.L. Su, Appl. Catal. A 243 (2003) 25–39.
[26] V. Idakiev, T. Tabakova, Z.-Y. Yuan, B.-L. Su, Appl. Catal. A 270 (2004) 135–141.
[27] Q. Fu, H. Saltsburg, M. Flytzani-Stephanopoulos, Science 301 (2003) 935–938.
[28] M. Haruta, B.S. Uphade, S. Tsubota, A. Miyamoto, Res. Chem. Intermed. 24 (1998) 329–336.
[29] R. Zanella, L. Delannoy, C. Louis, Appl. Catal. A 291 (2005) 62–72.
[30] M. Haruta, Cattech 6 (2002) 102–125.
[31] S.Q. Ma, G. Li, X.S. Wang, Chem. Lett. 35 (2006) 428–429.